Journal of Medicinal and Nanomaterials Chemistry 2 (2020) 138-147

Journal of Medicinal and Nanomaterials Chemistry

Journal homepage: https://jmnc.samipubco.com/

Short Communication

Enantiopure asymmetrically functionalized lambda-shape nanoscaffolds: optically active ethano-bridged hybrid Tröger base analogs

Masoud Kazem-Rostami

Faculty of Science and Engineering, Macquarie University, North Ryde, NSW 2109, Australia

ARTICLE INFORMATION

Received: 19 Agust 2019
Received in revised: 9 September 2019
Accepted: 12 September 2019
Available online: 10 February 2020

DOI: 10.48309/JMNC.2020.2.6

KEYWORDS

Tröger base
Enantioseparation
Nitrogen stereocenter
Chiral discriminator

ABSTRACT

Hybridization, functionalization, and enantioseparation of ethano-bridged Tröger base analogs have been performed. X-ray crystallographic analysis, chiral HPLC and CD spectroscopy have assigned the absolute configuration of the obtained ethano-bridged Tröger base analogs, confirming their optical purity. These optically active building blocks are readily modifiable and owing to their versatility they offer unique benefits for the growing community of molecular machinists.

Graphical Abstract

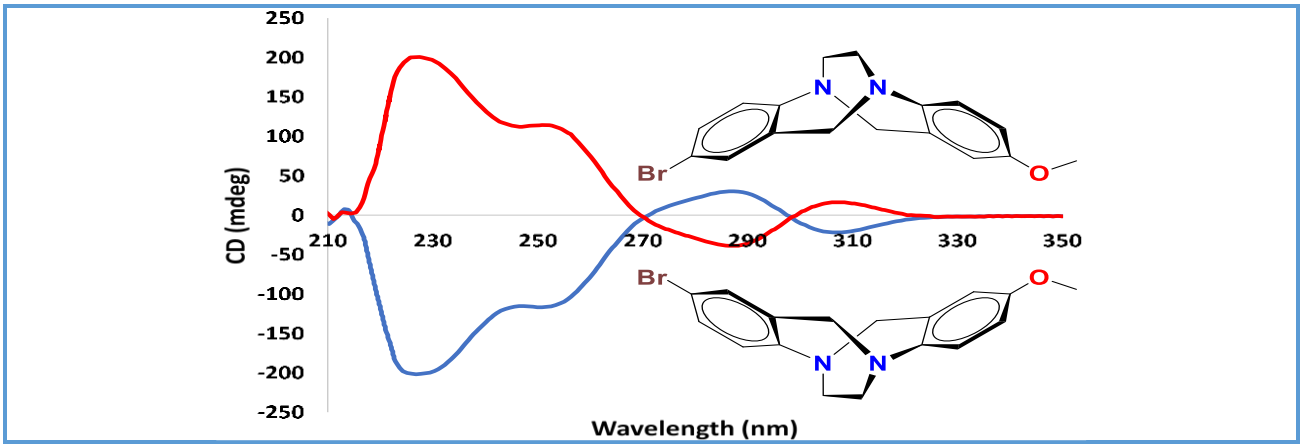

Introduction

Corresponding author, email: masoud.kazem-rotami@hdr.mq.edu.au (M. Kazem-Rostami).
Tel.: 0061 2 9850 8309; +61 2 9850 8309.

The rise of molecular machines [1, 2] has inspired the fusion of photoresponsive units with the lambda-shape scaffold of Tröger base analogs (TBAs) that has resulted in the introduction of light-driven nanoswitches (ranging from 8 to 64 Å in length) [3]. Despite the long history and broad range applications of both TBAs [4] and azo switches [5], no azo carrying TBA was ever fashioned until 2016 [6]. The unique lambda-shape geometry of TBAs can open new possibilities in the design of nanostructures including cyclophanes [7, 8], helicates [9, 10], molecular cleft receptors [11, 12], metal-organic frameworks and mechanically interlocked molecules [1].

The rigid scaffold of TBAs inhibits the pyramidal inversion of its nitrogen stereocenters, *i.e.* stereogenic amine groups, and determines an absolute *RR* or *SS* configuration [13]. Nevertheless, methano-bridged TBAs in the presence of protonating agents endure the pyramidal inversion and hence are prone to an acid-catalyzed racemization [14]. The racemization of methano-bridged TBAs can be prevented by the modification of the diazocine ring [15], *i.e.* replacing the methylene bridge with an ethylene bridge (Schemes 1), as Mukai and Hamada had introduced in 1996.

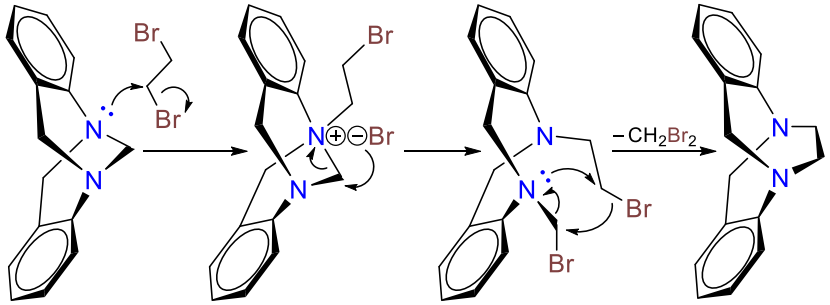

Scheme 1. Plausible mechanism of MHM transforming methano- to ethano-bridged TBAs

Ever since Mukai and Hamada's method (MHM) has created the first ethano-bridged analog of Tröger's base (Scheme 1) [16], a variety of innovative synthetic approaches have been developed including the rearrangement of ammonium salts [17], double aza-Michael addition [18], enantioselective [19, 20], and diastereoselective [21] insertion of carbenes. Although these methods are proven to be significantly efficient, even in the production of more complex structures [22], they require specialized reagents, result in functionalized straps and occasionally include a considerable amount of technicalities that altogether justify an occasional return to old-school MHM. Therefore, the present work employs MHM owing to its simplicity, accessibility, and scalability. This method swaps the diazocine bridges through the alkylation of methano-bridged TBAs with 1,2-dibromoethane (Scheme 1).

The enantiomeric resolution of TBAs has been achieved by high-performance liquid chromatography (HPLC) [23], capillary electrophoresis [24], and the formation of diastereomeric salt (or complex) using acidic chiral discriminators [15, 25]. The latter has been utilized in the present study due to its scalability and cost-efficiency.

Results and Discussion

In this work, methano-bridged TBAs **M1** (Scheme 2) and **M3–5** (Scheme 3), as precursors to the desired building blocks **1–5**, were first synthesized through the trögeration

reaction (TR) [14] between anilines and paraformaldehyde in trifluoroacetic acid [26]. The obtained methano-bridged TBAs **M1** and **M3–5** were then used, as starting material in MHM, for the production of the corresponding ethano-bridged TBAs **1** and **3–5**. The enantiomers of the resulting ethano-bridged TBAs **1**, **4** and **5** were then separated by their coprecipitation [15, 27] with enantiopure derivatives of tartaric acid. Despite numerous attempts, TBA **3** exceptionally did not form any diastereomeric salt (or complex) with the applied derivatives of tartaric acid; hence its enantioseparation (ES) failed through the coprecipitation. This failure is probably due to the existence of electronegative functional groups that may decrease the basicity of the bridgehead amine groups and weaken their interaction with the acidic chiral discriminators. Therefore, as a practical alternative, the separated enantiomers of TBA **1** were brominated to obtain enantiopure TBAs **2** and **3** (Scheme 2).

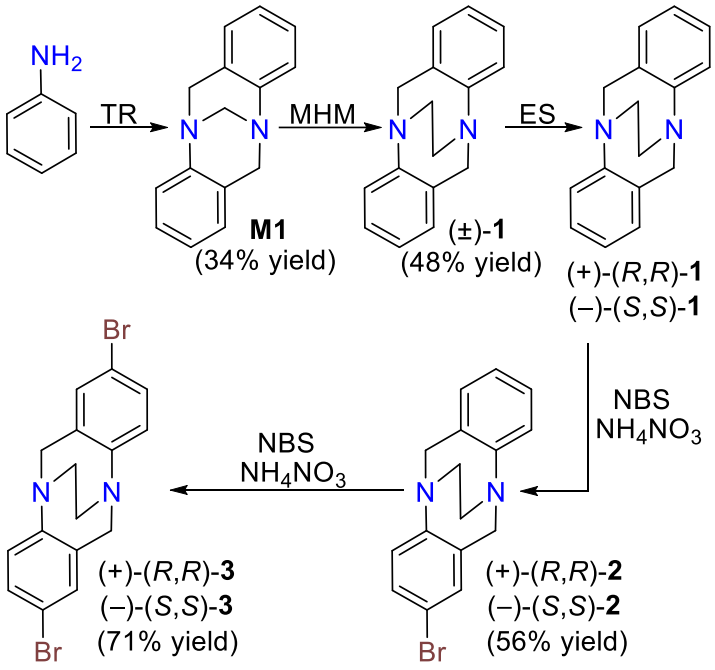

Scheme 2. Synthesis, enantiomeric resolution, and functionalization of optically active unsubstituted TBA **1**; TR: trögeration reaction of aniline with $OH(CH_2O)_nH$ in CF_3CO_2H [26]; MHM: $C_2H_4Br_2$ and Li_2CO_3 in DMF at 110 °C [16]; ES: enantioseparation with dibenzoyl tartaric acid in dry CH_3CN or $(CH_3)_2CO$ [27]; NBS: *N*-bromosuccinimide [28]

Unsubstituted TBA **1** is a versatile building block that can be conveniently modified, by a variety of electrophilic [29], and then nucleophilic [30], substitution reactions that can provide a broad spectrum of optically active lambda-shape building blocks. Nevertheless, the trögeration of unsubstituted aniline is considerably inefficient as it coincides with undesired condensation and polymerization reactions [31]. For example, the inevitable formation of aniline-formaldehyde-resin significantly decreases the trögeration yield of **M1** (TR, Scheme 2), increases the associated costs, and makes the work-up tedious. As an alternative, the hybridization strategy (Scheme 3) has been considered that doubles the total

trögeration yield while offering two more useful products.

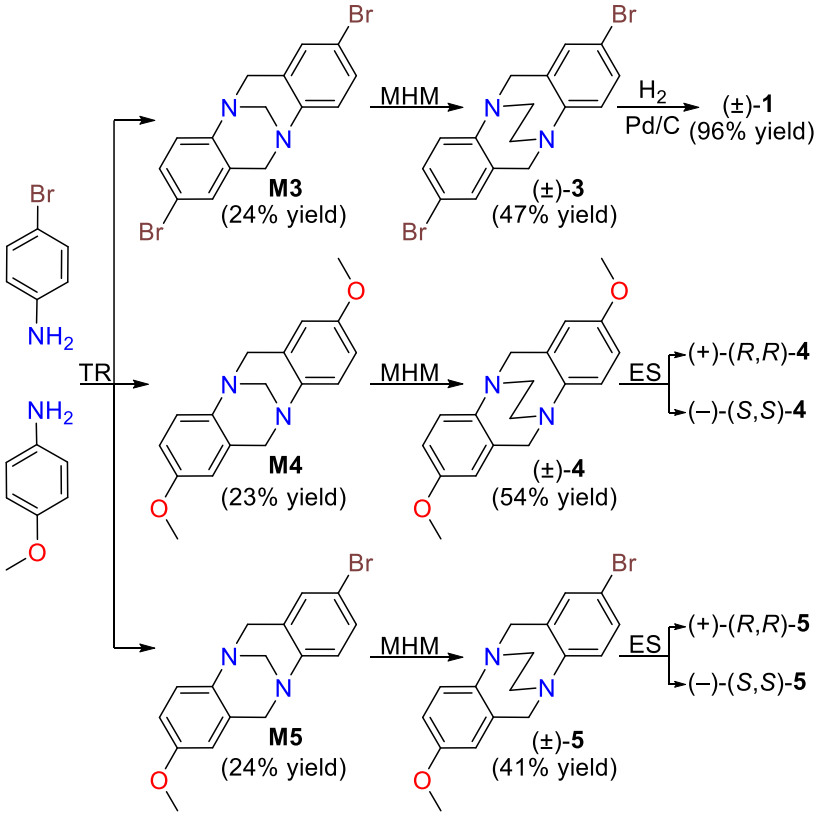

Scheme 3. One-pot synthesis of Tröger base analogs, their strap change, and enantioseparation

It is worth mentioning that, although the overall yield for the preparation of TBA **3** through both bromination of **1** (Scheme 2) and the hybridization method (Scheme 3) is 11–12%, the hybridization method yields the equal amounts of TBAs **4** and **5** (Scheme 3) where the synthesis of unsubstituted TBA **1** (Scheme 2) only leads to the undesired polymerization. The hybridization method (Scheme 3) eliminates the chances for the polymerization and guarantees an effortless work-up.

In the hybridization method (Scheme 3), bromo- and methoxy-carrying anilines were utilized owing to their significantly different chemistries that enable the modification of the resulting TBAs. The bromo and methoxy substituents can be readily converted to other functional groups and, owing to their location at 2 and 8 positions they can, provide excellent attachment/interaction sites (Scheme 4) [29, 32]. For instance, the methoxy substituents can be efficiently demethylated and be converted to hydroxyl groups (conversion yield > 97%) [13, 33, 34]. Hydroxyl groups can serve as attachment sites either via hydrogen or covalent bonds, *e.g.* be used in etherification, esterification, condensation or coupling reactions [6, 14, 15, 33, 34], or serve as ionizable groups making TBAs water-soluble [13]. Amongst halogenated TBAs, those carry bromo substituents are known as the best substrate for a variety of reactions including the amination of halogen carrying TBAs [35]. The bromo substituent can be used in various nucleophilic

substitution [36] and cross-coupling reactions [29, 30, 32, 37–40]. Moreover, bromo-carrying TBAs can be reduced back to unsubstituted TBAs, *e.g.* the reduction of **3** by $H_{2(g)}$/Pd-C (Scheme 3) gives **1** that is suitable for ES. Similarly, **5** could have been reduced to a monomethoxy TBA if needed.

As discussed, the hybridization method is mainly advantageous as far as the selected functional groups interact differently with the stationary phase(s) selected for the separation of the products. The retention and retardation factors of the brominated and methoxy-carrying TBAs are significantly different from one another, hence are conveniently separable using the ordinary silica packed chromatography columns. For example, R_f values for **M3**, **M5**, and **M4** (silica gel, DCM) are 0.46, 0.21, and 0.07; respectively. In addition, the righthanded enantiomers of **3**, **5**, and **4** only showed similar ^{t}R values where respectively 20, 30 and 40 % of a polar solvent (*i*PrOH) was blended in the mobile phase of the chiral HPLC. These indicated a significant increase in the polarity upon the introduction of the methoxy groups.

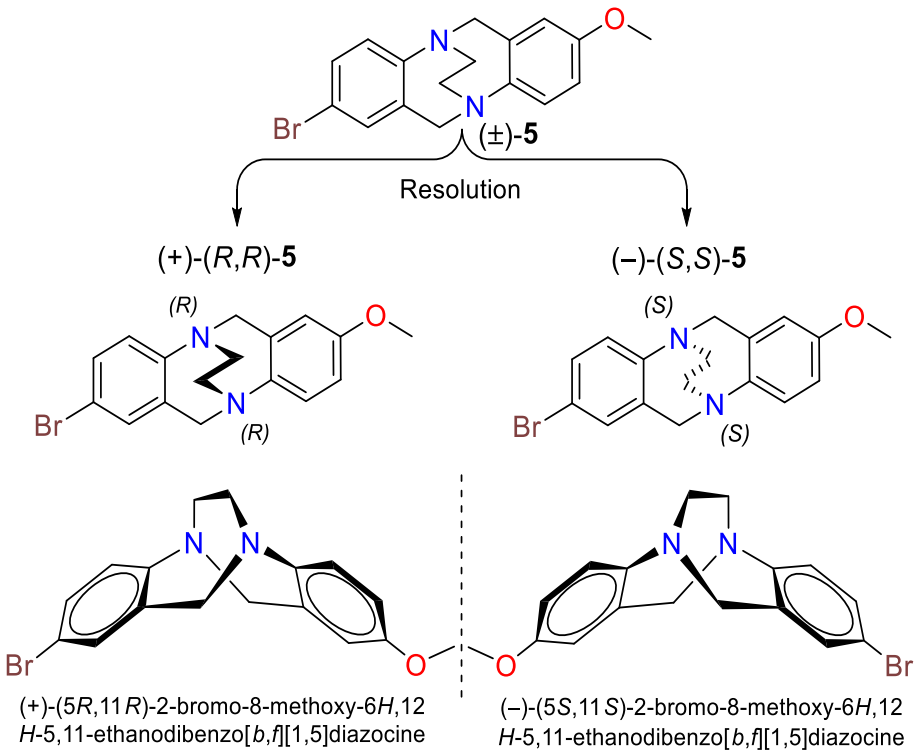

Scheme 4. Enantioseparation, mirror image presentation, and absolute configuration of (+)-(*R*,*R*)-**5** and (–)-(*S*,*S*)-**5** assigned according to X-ray crystallographic analysis (CCDC 1921569)

This study has also determined the absolute configuration, enantiopurity, and optical activity of the separated enantiomers of ethano-bridged TBAs **1**–**3** and **5** using X-ray crystallographic analysis, chiral HPLC and CD spectroscopy (Table 1).

Table 1. CD spectra of (+)-(*R*,*R*) and (–)-(*S*,*S*) enantiomers of **1**, **2**, **3** and **5** and stacked chiral HPLC chromatograms of their (±)-racemate (I), (+)-(*R*,*R*)-enantiomer (II), and (–)-(*S*,*S*)-enantiomer (III)

Compd.	CD spectra and chemical structure	Chiral HPLC chromatogram
1	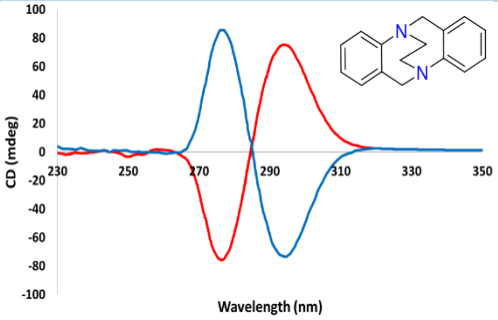	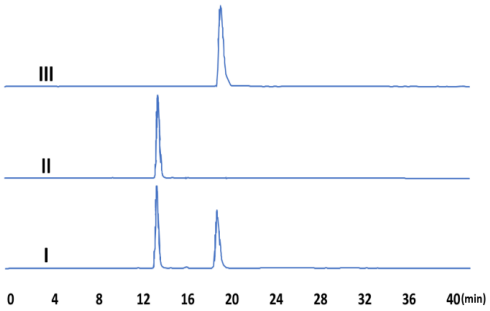
2	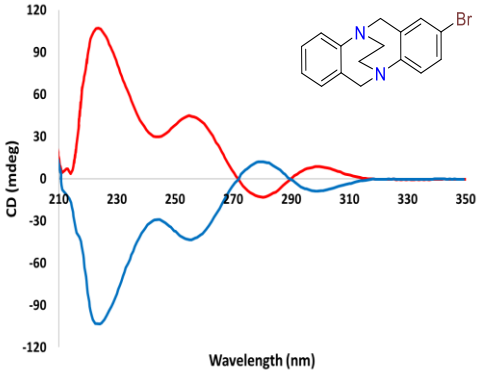	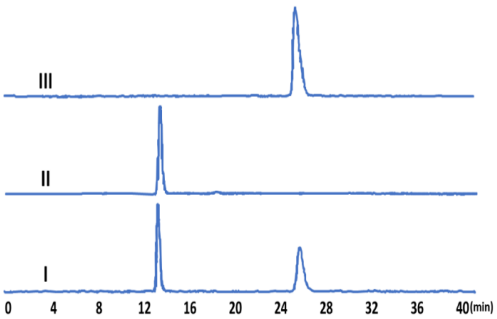
3	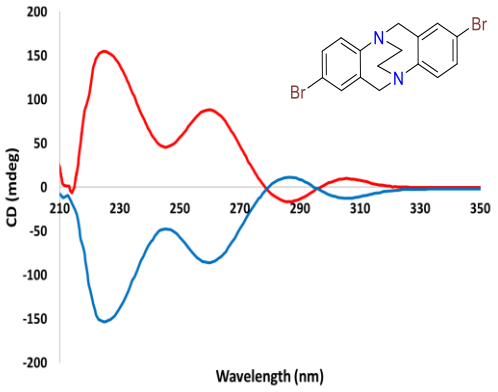	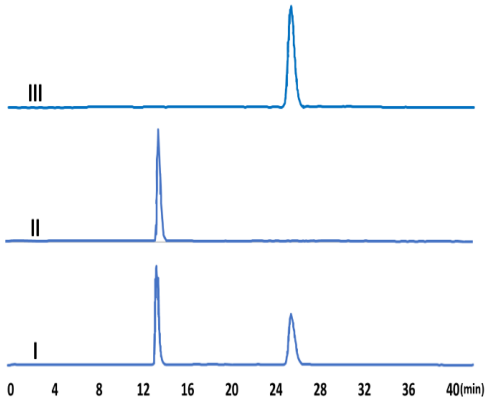
5	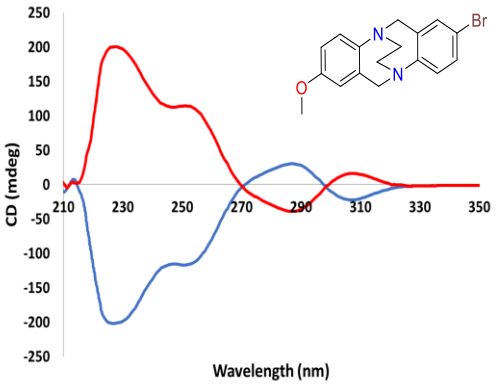	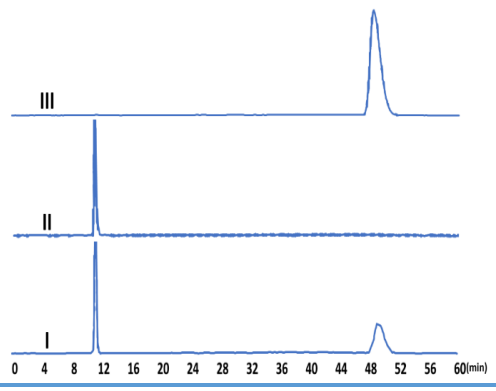

Experimental

Materials and methods

Agilent Quadrupole-6130 (HPLC-MS), Bruker DRX400 (NMR), Eppendorf Kinetic-Bio

(UV-Vis), Jasco J-810 (CD), Perkin-Elmer P-1010 (polarimeter), Shimadzu CTO-20A (HPLC) fitted with chiral analytical Daicel (Chiralpak-AD 250×4.6 mm, 5 µm) column, and Thermo Scientific Nicolet iS5/10 (ATR-IR), instruments were employed. Davisil LC60Å silica gel (40–63 µm), Merck DC-Kieselgel60-F_{254} aluminum TLC plates, and Spectroline UV lamp ENF-260 C/FE [230 V, 0.17 A, 50 Hz]-256 nm were used for chromatography.

*Procedures for the Preparation of Methano-Bridged TBAs **M1**–**M5***

Synthesis procedures and analytical data for methano-bridged TBAs **M1**–**M5** are available in the literature [26, 28, 36, 41, 42].

*Procedures for the Preparation of Ethano-Bridged TBAs **1**, **3** and **4***

Synthesis procedures and analytical data for ethano-bridged TBAs **1** and **3** in racemic form [43], and **4** in optically active form [15], are also available in the literature.

*Procedures for the Preparation of Optically Active TBAs **2** and **3***

Optically active TBAs **2** and **3** were obtained from the bromination of enantiopure TBA **1** using *N*-bromosuccinimide and ammonium nitrate. The detailed procedure is available in the literature [28, 44], and the required ratios of reactant to reagent for mono- and dibromination were 1:1 and 1:3 respectively. The mono-bromination reaction started with (+)-(*R*,*R*)-**1** and (–)-(*S*,*S*)-**1** gave (+)-(*R*,*R*)-**2** and (–)-(*S*,*S*)-**2**, respectively. The dibromination of (+)-(*R*,*R*)-**1** and (–)-(*S*,*S*)-**1** gave (+)-(*R*,*R*)-**3** and (–)-(*S*,*S*)-**3**, respectively.

*Characterization of Ethano-Bridged TBA **2***

Started with enantiopure TBA **1** (0.24 g, 1.0 mmol) adopting Sergeyev's method to obtain **2** as an off-white solid [28]. Yield 0.13 g (56%, 0.56 mmol), R_f 0.5 (Silica gel/EtOAc-DCM 15% v/v). ^{1}H NMR (400 MHz, $CDCl_3$): δ 7.01–7.15 (m, 4 H), 6.79–7.01 (m, 3 H), 4.59 (d, J = 17.1 Hz, 1 H), 4.54 (d, J = 17.1 Hz, 1 H), 4.40 (d, J = 17.1 Hz, 1 H), 4.37 (d, J = 17.1 Hz, 1 H), 3.46–3.71 (m, 4 H). ^{13}C NMR (100 MHz, $CDCl_3$): δ 150, 149.6, 138.9, 136.5, 131.5, 130.0, 129.8, 128.6, 127.9, 127.2, 125.1, 117.8, 59.1, 58.9, 54.6, 54.5. MS (ESI +, Quadrupole): *m/z* [M + H]$^+$ calcd for $[C_{16}H_{16}BrN_2]^+$: 315.04; found: 315.1 and 317.2. IR (neat): 2905, 1516, 1481, 1342, 1218, 1089, 945 cm^{-1}. Anal. Calcd for $C_{16}H_{15}BrN_2$: C, 60.97; H, 4.80; N, 8.89. Found: C, 61.15; H, 4.97; N, 9.03.

*Preparation and Characterization of Hybrid Ethano-Bridged TBA **5***

Methano-bridged TBA **M5** (1.65 g, 5.0 mmol, 1.0 equiv.), 1,2-dibromoethane (2.35 g, 12.5 mmol, excess), DMF (25 mL) and Li_2CO_3 (1.8 g, 25.0 mmol, excess) were mixed in an oven dried round bottom flask and heated at 105 °C for 12 h under argon atmosphere in darkness. DMF was removed under reduced pressure; the remaining residue was dissolved in EtOAc (30 mL) and thoroughly rinsed with distilled water (50 mL × 5), dried over sodium sulfate, filtered and evaporated under reduced pressure. The collected crude was chromatographed to obtain ethano-bridged TBA **5** as an off-white solid. Yield 0.70 g (41% 2.0 mmol); R_f 0.5 (Silica gel/ EtOAc-DCM 25% v/v). ^{1}H NMR (400 MHz, $CDCl_3$): δ 7.15–7.18 (m, 1 H), 6.96–7.08 (m, 3 H), 6.40–6.64 (m, 2H), 4.49–4.58 (m, 2H), 4.28–4.41 (m, 2 H), 3.70 (s, 3 H), 3.47–3.65 (m, 4 H). ^{13}C NMR (100 MHz, $CDCl_3$): δ 166.1, 156.5, 149.3, 138.9, 137.4, 131.5, 130.3, 129.8, 128.7, 117.5, 113.4, 112.7, 59.1, 58.9,55.1, 54.9, 54.8. MS (ESI +, Quadrupole): *m/z* [M + H]$^+$ calcd for $[C_{17}H_{18}BrN_2O]^+$: 345.06; found: 345.1 and 347.1. IR (neat): 2903, 2361, 1490, 1471, 1275, 1065, 1023, 842 cm^{-1}. Mp: 154–156°C. Anal. Calcd for $C_{17}H_{17}BrN_2O$: C, 59.14; H, 4.96; N, 8.11. Found: C,

59.23; H, 5.12; N, 7.93. CCDC Deposition Number 1921569.

*Enantiomeric Resolution and Optical Activity of Ethano-Bridged TBAs **1**–**3**, and **5***

The procedure reported by Jameson *et. al.* [27], was slightly modified and employed for the enantiomeric resolution of TBAs **1**–**3** and **5** that coprecipitated with enantiopure *O,O′*-dibenzoyl-tartaric acid (Mole ratio of 1:3 respectively) in dry CH_3CN or $(CH_3)_2CO$ and recrystallized twice in fresh solvent before the work-up. This resulted in the chiral resolution of eight enantiomers, as follows:

Enantiomer (+)-(*R*,*R*)-**1**: $[\alpha]_D^{22}$ +378 (*c* 0.1), Chiral HPLC ^tR 13 ± 1 min (major >99.8%, er >99.5:0.5); Enantiomer (–)-(*S*,*S*)-**1**: $[\alpha]_D^{18}$ –361 (*c* 0.1), Chiral HPLC ^tR 19 ± 1 min (major >99.4%, er >99.5:0.5); mobile phase: *i*PrOH – *n*Hex, 10% *v*/*v*.

Enantiomer (+)-(*R*,*R*)-**2**: $[\alpha]_D^{21}$ +453 (*c* 0.1), Chiral HPLC ^tR 13 ± 1 min (major >98.4%, er >99.5:0.5); Enantiomer (–)-(*S*,*S*)-**2**: $[\alpha]_D^{24}$ –468 (*c* 0.1), Chiral HPLC ^tR 26 ± 2 min (major >98.6%, er >99.5:0.5); mobile phase: *i*PrOH – *n*Hex, 15% *v*/*v*.

Enantiomer (+)-(*R*,*R*)-**3**: $[\alpha]_D^{22}$ +429 (*c* 0.1), Chiral HPLC ^tR 13 ± 1 min (major >99.8%, er >99.5:0.5); Enantiomer (–)-(*S*,*S*)-**3**: $[\alpha]_D^{19}$ –440 (*c* 0.1), Chiral HPLC ^tR 25 ± 1 min (major >99.6%, er >99.5:0.5); mobile phase: *i*PrOH – *n*Hex, 20% *v*/*v*.

Enantiomer (+)-(*R*,*R*)-**5**: $[\alpha]_D^{20}$ +524 (*c* 0.1), Chiral HPLC ^tR 11 ± 1 min (major >99.8%, er >99.5:0.5); Enantiomer (–)-(*S*,*S*)-**5**: $[\alpha]_D^{23}$ –516 (*c* 0.1), Chiral HPLC ^tR 49 ± 3 min (major >99.8%, er >99.5:0.5); mobile phase: *i*PrOH – *n*Hex, 30% *v*/*v*; CCDC Deposition Number 1921569.

Conclusions

As discussed, there has been a trade-off between the functionalization and the hybridization methods. Functionalization of the enantiopure unsubstituted TBA includes a wasteful initial step, although presents a versatile building block. The hybridization method doubles the initial yield while introduces some additional levels of technicality for the separation of the products and their optical resolution. Regardless of the chosen strategy, the obtained lambda-shape enantiomers are ideal nanoscale building blocks for the growing community of molecular machinists [2]. These molecules can be equipped with photoswitchable units [15], interlinking and interactive extremities; *e.g.* halogen- or hydrogen-bond donor and acceptor groups [6, 14]. The resulting stimuli-responsive lambda-shape linkers are expected to provide tight control over their tunable assembly, chelation, homodimerization or macrocyclization, liquid crystalline [45] and binding [46-48] behaviors. Such molecules can also be used as molecular recognition agents and chiral discriminators [49] as the possibilities for the customization of such functionalized TBAs are endless.

Acknowledgements

The financial aid of the Australian Government (Research Training Program Scholarship: IPRS2014-004) and Macquarie University (HDR43010477 and PGRF2016-R2-1672525) from 2014 to 2017 are gratefully acknowledged. Mr Mark Tran and Assoc Prof Andrew Carl Try are thanked for the provided technical assistance and initiatives, respectively.

Orcid

Masoud Kazem-Rostami 0000-0003-4821-5820

Supporting Information

Additional supporting information related to this article can be found, in the online version, at DOI: 10.26655/AJNANOMAT.2020.2.6.

Accession Codes

CCDC 1921569 contains crystallographic data for this work. These data can be obtained free of charge via www.ccdc.cam.ac.uk (or from the Cambridge Crystallographic Data Center, 12, Union Road, Cambridge CB2 1EZ, UK; fax: +441223 336033).

References

[1]. Stoddart J.F. *Angew. Chem. Int. Ed*., 2017, **56**:11094
[2]. Sluysmans D., Stoddart J.F. *Proc. Natl. Acad. Sci. U.S.A*., 2018, **115**:9359
[3]. Kazem-Rostami M., Akhmedov N.G., Faramarzi S. *J. Mol. Struct*., 2019, **1178**:538
[4]. Dolenský B., Elguero J., Král V., Pardo C., Valík M., *Current Tröger's Base Chemistry*. In Adv. Heterocycl. Chem.; Academic Press: United States, 2007; p 56
[5]. Bandara H.M.D., Burdette S.C. *Chem. Soc. Rev*., 2012, **41**:1809
[6]. Kazem-Rostami M. *Synthesis*, 2017, **49**:1214
[7]. Cowart M.D., Sucholeiki I., Bukownik R.R., Wilcox C.S. *J. Am. Chem. Soc*., 1988, **110**:6204
[8]. Cai K., Lipke M.C., Liu Z., Nelson J., Cheng T., Shi Y., Cheng C., Shen D., Han J.-M., Vemuri S., Feng Y., Stern C.L., Goddard W.A., Wasielewski M.R., Stoddart J.F. *Nat. Commun*., 2018, **9**:5275
[9]. Kiehne U., Weilandt T., Lützen A. *Eur. J. Org. Chem*., 2008, **2008**:2056
[10]. Kiehne U., Weilandt T., Lützen A. *Org. Lett*., 2007, **9**:1283
[11]. Bhaskar Reddy M., Shailaja M., Manjula A., Premkumar J.R., Sastry G.N., Sirisha K., Sarma A.V.S. *Org. Biomol. Chem*., 2015, **13**:1141
[12]. Boyle E.M., Comby S., Molloy J.K., Gunnlaugsson T. *J. Org. Chem*., 2013, **78**:8312
[13]. Kazem-Rostami M. *Synlett*, 2017, **28**:1641
[14]. Kazem-Rostami M., Moghanian A. *Org. Chem. Front*., 2017, **4**:224
[15]. Kazem-Rostami M. *New J. Chem*., 2019, **43**:7751
[16]. Hamada Y., Mukai S. *Tetrahedron Asymmetry*, 1996, **7**:2671
[17]. Michon C., Sharma A., Bernardinelli G., Francotte E. *Lacour J. Chem. Commun*., 2010, **46**:2206
[18]. Kamiyama T., Sigrist L., Cvengroš J. *Synthesis*, 2016, **48**:3957
[19]. Sharma A., Besnard C., Guenee L. *Lacour J. Org. Biomol. Chem*., 2012, **10**:966
[20]. Sharma A., Guenee L., Naubron J.-V. *Lacour J. Angew. Chem., Int. Ed*., 2011, **50**:3677
[21]. Bosmani A., Guarnieri-Ibáñez A. *Lacour J. Helv. Chim. Acta*, 2019, **102**:1900021
[22]. Alessandro B., Alejandro G.I., Sébastien G., Céline B. *Jérôme L. Angew. Chem. Int. Ed*., 2018, **57**:7151
[23]. Michon C., Gonçalves-Farbos M.-H. *Lacour J. Chirality*, 2009, **21**:809
[24]. Weatherly C.A., Na Y.-C., Nanayakkara Y.S., Woods R.M., Sharma A., Lacour J., *Armstrong D.W. J. Chromatogr. B*, 2014, **955**:72
[25]. Satishkumar S., Periasamy M. *Tetrahedron Asymmetry*, 2006, **17**:1116
[26]. Didier D., Tylleman B., Lambert N., Vande Velde C.M.L., Blockhuys F., Collas A., Sergeyev S. *Tetrahedron*, 2008, **64**:6252
[27]. Jameson D.L., Field T., Schmidt M.R., DeStefano A.K., Stiteler C.J., Venditto V.J., Krovic B., Hoffman C.M., Ondisco M.T., Belowich M.E. *J. Org. Chem*., 2013, **78**:11590
[28]. Didier D., Sergeyev S. *Eur. J. Org. Chem*., 2007, **2007**:3905
[29]. Jensen J., Tejler J., Wärnmark K. *J. Org. Chem*., 2002, **67**:6008

[30]. Jarzebski A., Bannwarth C., Tenten C., Benkhaeuser C., Schnakenburg G., Grimme S. *Lützen A. Synthesis*, 2015, **47**:3118
[31]. Bishop R.R. *J. Appl. Chem*., 1956, **6**:256
[32]. Kiehne U., Lützen A. *Synthesis*, 2004, **2004**:1687
[33]. Tatar A., Valík M., Novotná J., Havlík M., Dolenský B., Král V., Urbanová M. *Chirality*, 2014, **26**:361
[34]. Malik Q.M., Ijaz S., Craig D.C., Try A.C. *Tetrahedron*, 2011, **67**:5798
[35]. Artacho J., Wärnmark K. *Synthesis*, 2009, **2009**:3120
[36]. Dusso D., Ramirez C., Parise A., Lanza P., Vera D.M., Chesta C., Moyano E.L., Akhmedov N.G. *Magn. Reson. Chem*., 2019, **57**:423
[37]. Didier D., Sergeyev S. *Tetrahedron*, 2007, **63**:3864
[38]. Benkhäuser-Schunk C., Wezisla B., Urbahn K., Kiehne U., Daniels J., Schnakenburg G., Neese F., Lützen A. *ChemPlusChem*, 2012, **77**:396
[39]. Weilandt T., Kiehne U., Bunzen J., Schnakenburg G., Lützen A. *Chem. Eur. J*., 2010, **16**:2418
[40]. Kiehne U., Bruhn T., Schnakenburg G., Fröhlich R., Bringmann G., Lützen A. *Chem. Eur. J*., 2008, **14**:4246
[41]. Ishida Y., Ito H., Mori D., Saigo K. *Tetrahedron Lett*., 2005, **46**:109
[42]. Faroughi M., Zhu K.-X., Jensen P., Craig D.C., Try A.C. *Eur. J. Org. Chem*., 2009, **2009**:4266
[43]. Pereira R., Pfeifer L., Fournier J., Gouverneur V., Cvengroš J. *Org. Biomol. Chem*., 2017, **15**:628
[44]. Sergeyev S., Didier D., Boitsov V., Teshome A., Asselberghs I., Clays K., Vande Velde C.M.L., Plaquet A., Champagne B. *Chem. Eur. J*., 2010, **16**:8181
[45]. Kazem-Rostami M. *J. Therm. Anal. Calorim*., 2019,
[46]. Maugeri L., Lébl T., Cordes D.B., Slawin A.M.Z., Philp D. *J. Org. Chem*., 2017, **82**:1986
[47]. Maugeri L., Jamieson E.M.G., Cordes D.B., Slawin A.M.Z., Philp D. *Chem. Sci*., 2017, **8**:938
[48]. Maugeri L., Asencio-Hernández J., Lébl T., Cordes D.B., Slawin A.M.Z., Delsuc M.-A., Philp D. *Chem. Sci*., 2016, **7**:6422
[49]. Banerjee S., Bright S.A., Smith J.A., Burgeat J., Martinez-Calvo M., Williams D.C., Kelly J.M., Gunnlaugsson T. *J. Org. Chem*., 2014, **79**:9272

How to cite this manuscript: Masoud Kazem-Rostami*. Enantiopure asymmetrically functionalized lambda-shape nanoscaffolds: optically active ethano-bridged hybrid Tröger base analogs. *Journal of Medicinal and Nanomaterials Chemistry*, 2(2) 2020, 138-147. DOI: 10.48309/JMNC.2020.2.6